ISSN:2372-0743 print
ISSN:2373-2989 on line
International Journal of Ground Sediment & Water
Vol. 05
2017

◆Research Paper◆

Numerical Transient Analysis of Pressure in Petroleum Reservoir

Pedro Victor Serra Mascarenhas[1], André Luís Brasil Cavalcante[1]
1. *University of Brasilia, Brasilia ,70910-900, Brazil*
E-mail:pvsmascarenhas@gmail.com; abrasil@unb.br

Abstract: This work regards oil flow in petroleum reservoirs. It is an analysis that aims the study of monophasic oil flow in porous media through the Diffusivity Equation's analytical solution for a radial, transient flow when varying reservoir and fluid parameters. This solution is especially important for preliminaries studies of petroleum reservoir regarding its economic and technical production viability for a qualitative understanding of the flow in the reservoir. In addition, a numerical model based on the Finite Difference Method (FDM) is implemented to solve the radial flow and relax the simplifying hypothesis used to solve the governing equation analytically. The numerical, more realistic, solution is compared to the analytical solution and the effects of the simplifying hypotheses of the model are further discussed.

Keywords: Transient Analysis, Finite Difference Method, Petroleum Reservoir, Diffusivity Equation, Analytical Analysis

1. Introduction

Recent oil barrel values drop to low prices demanded more efficient and reliable viability studies. It is possible to minimize risks and avoid bad capital investment through preliminary studies and a better understanding of how each fluid and geological variable influences the flow.

The paper begins with of the background theory used to study flow in porous media, where the Continuity Equation, equations of state and Darcy's Law are briefly discussed. By imposing the correct boundary conditions, these equations are combined to obtain the Diffusivity Equation, which is solved analytically to obtain an equation capable of describing pressure values at every point and time of the reservoir using geological and fluid information. Following that, the FDM model equations' are presented and its implementation is further discussed. In order to accomplish this, Mathematica Wolfram [1] computer language is chosen as the computational tool.

The numerical model is especially useful to study real geometry and parameters cases when obtaining an analytical equation without simplifying assumptions is not possible.

2. Deriving the Diffusivity Equation

The Diffusivity Equation's solution describes the pressure behavior with respect to the distance to the wellbore's center and time passed since the start of the production, and it is used in analysis well test data [2]. It is obtained by combining three sets of equations: one that describes the linear momentum conservation (Darcy's Law), one that describes the mass conservation (Continuity Equation) and equations that relate state variables, such as volume, pressure, temperature and mass (equations of state). The following topics are dedicated to introduce these equations, as well as the hypotheses behind their application.

Darcy's Law: the Conservation of Linear Momentum Equation. Henry Darcy first wrote Darcy's Law in 1856. It is an equation that describes the flow of fluid through porous media using the concept of the linear momentum conservation [3]. It was obtained empirically when Darcy first wrote this equation, but later it was derived from the Navier-Stokes equation for stationary, creeping and incompressible flow [4]. Darcy's Law is widely used in reservoir engineering for modeling flow in porous media, and those who intend to use it should understand its hypotheses: Darcy's Law is valid for incompressible, laminar flow, negligible inertial effects, and the viscous part of the strength tensor behaves according to Newton's Second Law for fluids [4].

$$v = -\frac{k\gamma}{\mu}\frac{d\Phi}{dl} \tag{1}$$

where γ denotes the fluid's specific weight [$ML^{-2}T^{-1}$]; μ denote the fluid's viscosity [$ML^{-1}T^{-1}$]; k denotes the porous medium's intrinsic permeability [L^2]; v is the fluid's instantaneous velocity [LT^{-1}]; l is the direction of the fluid's trajectory [L]; Φ denotes the fluid flow potential [L]. The fluid potential is the negative integral of the force over the path taken by an infinitesimally small volume of fluid when it moves from a reference location to the point under consideration [4]. It is a measure of the specific potential energy stored within the fluid. Thus,

$$\Phi = \int_{p_o}^{p} \frac{dp}{\gamma} + \left(Z - Z_o\right) \tag{2}$$

where p denotes the pressure [$ML^{-1}T^{2}$]; Z denotes the height with respect to a chosen datum [L] and the subindex "o" denotes reference values for the variables that it follows.

The derivative of the fluid potential with respect to the path the fluid takes is:

$$\frac{d\Phi}{dl} = \frac{1}{\gamma}\frac{dp}{dl} + \frac{dZ}{dl} \tag{3}$$

Continuity Equation: The Mass Conversation Equation. The Continuity Equation states physically that the variation of fluid mass in a control volume within time is equal to the balance of fluid that flow inward and outwards of the volume plus any source within that volume, or diminished any sink that might be present inside the volume. The source/sink flow term is useful to model internal boundary conditions of

specified flow rates (i.e. injection or removal of hydrocarbonates through a well). The Continuity Equation is written as it follows[5]:

$$\nabla \cdot (v\rho) + \frac{\rho_{std} q_{sc}}{V_b} = -\frac{\partial(\phi\rho)}{\partial t} \tag{4}$$

where ρ denotes the fluid's specific mass [ML^{-3}]; V_b is the bulk volume [L^3]; ϕ is the medium's porosity [non-dimensional]; t is the time [T]; q_{sc} [L^3T^{-1}] is the source/sink rate term and the sub-index std stands for variables at standard pressure and temperature conditions.

Equations of State. Equations of state are any constitutive laws that relate pressure, temperature, volume and mass for a given fluid. One much-known example of an equation of state is the Ideal Gas Law[3].

The importance of equations of state on the model is that they can be used to replace variables on the Diffusivity Equation by variables usually measured on field evaluations and variables that are easier to work with. Two important equations are going to be used for this purpose, fluid compressibility equation and rock formation compressibility equation, both specified for isothermal analysis. The fluid compressibility equation is defined as the percentage of the total volume that the volume variation rate with the pressure represents:

$$c = -\frac{1}{V}\left(\frac{\partial V}{\partial p}\right) \tag{5}$$

where c is the fluid's isothermal compressibility [$M^{-1}LT^{-2}$] and V is the volume [L^3].

One may write Equation (5) on the form that is more useful to the current purpose using the definition of specific mass:

$$c = \frac{1}{\rho}\left(\frac{\partial \rho}{\partial p}\right) \tag{6}$$

The Equation (6) may also be used to write relations between specific mass and pressure spatial partial derivatives and specific mass and pressure time partial derivatives. These equations are:

$$\nabla \cdot p = \frac{1}{\rho c} \nabla \cdot \rho \tag{7}$$

and

$$\rho \frac{\partial p}{\partial t} = \frac{1}{c} \frac{\partial \rho}{\partial t} \tag{8}$$

The other equation of state, the rock formation compressibility, is the percentage of the rock porosity that the variation of porosity with respect to the pressure represents [3]:

$$c_f = \frac{1}{\phi}\left(\frac{\partial \phi}{\partial p}\right) \tag{9}$$

Mathematical manipulations may as well allow Equation (9) to be written on a

way that may be applied to the model:

$$\frac{\partial p}{\partial t} = \frac{1}{\phi c_f}\frac{\partial \phi}{\partial t} \tag{10}$$

The sum of the two compressibilities showed on the text is called the total compressibility:

$$c_t = c + c_f \tag{11}$$

It is also useful to use the defined compressibilities to obtain equations that allow to calculate porosity and oil formation volume factor for different times since the beginning of the production [5]:

$$B = \frac{B_o}{1 + c\left(p - p_o\right)} \tag{12}$$

$$\phi = \phi_o\left[1 + c_f\left(p - p_o\right)\right] \tag{13}$$

where B is the oil formation volume factor [non-dimensional].

The Diffusivity Equation and its Solution. Equation (4) can be fully expanded with respect to the space variables:

$$\begin{aligned}\frac{\partial}{\partial x}\left(\frac{\rho k_x}{\mu}\frac{\partial p}{\partial x}\right) + \frac{\partial}{\partial y}\left(\frac{\rho k_y}{\mu}\frac{\partial p}{\partial y}\right) + \frac{\partial}{\partial z}\left(\frac{\rho k_z}{\mu}\frac{\partial p}{\partial z}\right) + \frac{\rho_{std} q_{sc}}{V_b} = \\ \frac{\partial}{\partial x}\left(\frac{\rho k_x}{\mu}\gamma\frac{\partial Z}{\partial x}\right) + \frac{\partial}{\partial y}\left(\frac{\rho k_y}{\mu}\gamma\frac{\partial Z}{\partial y}\right) + \frac{\partial}{\partial z}\left(\frac{\rho k_z}{\mu}\gamma\frac{\partial Z}{\partial z}\right) + \frac{\partial(\phi\rho)}{\partial t}\end{aligned} \tag{14}$$

where the subindexes x, y and z denotes the Cartesian direction on in the space [L].

The source/sink term is not necessary to solve Equation (14) analytically, because it is redundant after applying boundary conditions. Therefore it may be considered zero. Rewriting Equation (14) into cylindrical coordinates:

$$\begin{aligned}\frac{1}{r}\frac{\partial}{\partial r}\left(r\frac{k_r}{\mu B}\frac{\partial p}{\partial r}\right) + \frac{1}{r^2}\frac{\partial}{\partial \theta}\left(\frac{k_\theta}{\mu B}\frac{\partial p}{\partial \theta}\right) + \frac{\partial}{\partial z}\left(\frac{k_z}{\mu B}\frac{\partial p}{\partial z}\right) = \\ \frac{1}{r}\frac{\partial}{\partial r}\left(r\frac{k_r}{\mu B}\gamma\frac{\partial Z}{\partial r}\right) + \frac{1}{r^2}\frac{\partial}{\partial \theta}\left(\frac{k_\theta}{\mu B}\gamma\frac{\partial Z}{\partial \theta}\right) + \frac{\partial}{\partial z}\left(\frac{k_z}{\mu B}\gamma\frac{\partial Z}{\partial z}\right) + \frac{\phi c_t}{B}\frac{\partial p}{\partial t}\end{aligned} \tag{15}$$

where the sub-indexes r, θ and z are the cylindrical grid directions, r is the radial direction variable [L], θ is the angular direction variable [non-dimensional] and z is the depth direction variable [L].

Some important hypotheses are assumed in order to obtain the analytical solution. It is assumed that the rock is homogeneous and isotropic, the fluid's viscosity is constant, fluid and rock compressibilities are small and constant, the fluid is isothermal and pressure gradients are small. It is also assumed that the flow is radial (i.e. no vertical pressure gradients) and transient (the reservoir behaves as if it is infinite and boundary conditions are not felt immediately along the reservoir extension. Equation (15) becomes:

$$\frac{1}{r}\frac{\partial}{\partial r}\left(r\frac{\partial p}{\partial r}\right)=\frac{1}{\eta}\frac{\partial p}{\partial t} \tag{16}$$

where the rock and fluid parameters were replaced by the diffusivity constant [2]:

$$\eta=\frac{k}{\phi\mu c_t} \tag{17}$$

It is necessary to specify properly three boundary conditions to solve Equation (16) [2]:

- It is assumed that, at $t = 0$, the pressure inside the reservoir is constant $p(r;0) = p_{t=0}$, $r>0$.
- It is assumed that if a point sufficiently far is taken, its pressure is equal to the initial pressure $lim[p(r,t)]_{r\to\infty}= p_{t=0}$.
- It is assumed that the flow rate inside the wellbore is constant $q_w=cte$.

Furthermore, the last boundary condition may be written as it follows using Darcy's Equation and taking its limit with r→∞:

$$\lim_{r\to 0}\left(r\frac{\partial p}{\partial r}\right)=\frac{q_w\mu}{2\pi kh} \tag{18}$$

where q_w is the well rate and h is the reservoir width [L^3T^{-1}].

One may find the pressure equation along the reservoir [3] using these boundary conditions and solving Equation (16):

$$p(r,t)=p_{t=0}-\frac{q_w\mu}{4\pi kh}E_i\left(\frac{\phi\mu c_t r^2}{4kt}\right) \tag{19}$$

where $E_i(X)$ is the integral exponential function, defined as follows [3]:

$$E_i(X)=\int_X^\infty\frac{e^{-\xi}}{\xi}d\xi \tag{20}$$

Finite Difference Method Model. There are three most commonly used numerical methods for reservoir simulation. These are Finite Element Method, Finite Difference Method and the Finite Volume Method [6]. Each of them has its advantages and disadvantages. The chosen method for this paper is the Finite Difference Method, which is the most traditional numerical method on fluid flow studies and its pros and cons are summarized in Table 1.

The FDM method is chosen to be implicit with a radial and geometrically growing grid. The grid grows following the rule:

$$r_{i+1}=\alpha_{lg}r_i \tag{21}$$

where α_{lg} is the mesh growth factor [non-dimensional].

In order to keep the discrete and continuous form of the Darcy Equation, the borders of the cells must be positioned according to the formula:

Table 1. Advantages and Disadvantages of the Finite Difference Method.

Finite Difference Method[6]	
Advantages	**Disadvantages**
Easy to write codes; Easy 3D extension; Good compatibility of physical aspects of fluid flow in porous medium	Highly dependent on the mesh; Difficult to implement for complicated geometry; big numerical dispersion associated with truncation; poor precision for a heterogeneous medium with high capillary pressure variations.

$$r_{i+1/2} = \frac{r_{i+1} - r_i}{\ln\left(\frac{r_{i+1}}{r_i}\right)} \tag{22}$$

The FDM formulation used here is developed in [5]. The implicit in time formulation is used, since the mesh is radial and it grows geometrically. The final equation that describes the method is:

$$\begin{aligned} &A^n_{i,j,k} p^{n+1}_{i,j,k+1} + B^n_{i,j,k} p^{n+1}_{i,j,k-1} + N^n_{i,j,k} p^{n+1}_{i,j+1,k} + S^n_{i,j,k} p^{n+1}_{i,j-1,k} + W^n_{i,j,k} p^{n+1}_{i+1,j,k} \\ &+ E^n_{i,j,k} p^{n+1}_{i-1,j,k} + C^{n+1}_{i,j,k} p^{n+1}_{i,j,k} = Q^n_{i,j,k} \end{aligned} \tag{23}$$

with,

$$A^n_{i,j,k} = T^n_{i,j,k+1/2} \tag{24}$$

$$B^n_{i,j,k} = T^n_{i,j,k-1/2} \tag{25}$$

$$N^n_{i,j,k} = T^n_{i,j+1/2,k} \tag{26}$$

$$S^n_{i,j,k} = T^n_{i,j-1/2,k} \tag{27}$$

$$W^n_{i,j,k} = T^n_{i-1/2,j,k} \tag{28}$$

$$E^n_{i,j,k} = T^n_{i+1/2,j,k} \tag{29}$$

$$C^{n+1}_{i,j,k} = -\left(A^n_{i,j,k} + B^n_{i,j,k} + N^n_{i,j,k} + S^n_{i,j,k} + W^n_{i,j,k} + E^n_{i,j,k} + \frac{\Gamma^{n+1}_{i,j,k}}{\Delta t} \right) \tag{30}$$

Each of these coefficients is a combination of transmissibilities through the face of two neighboring cell. The letters stand for the position of the cells in relation to the cell in analysis: above, below, north, west, east, south and center. Each of these coefficients shows how the pressure of cell itself and the pressure from neighboring cells are changing the pressure calculated.

The transmissibility is defined as:

Table 2. Expressions applied to Equation (31) to calculate the geometrical factor G [7].

Grid types and flow direction	Geometrical Factor ($G_{i+1/2}$)	Geometrical Factor ($G_{i-1/2}$)
Cylindrical, radial	$\frac{\Delta\theta_j \Delta z_k}{\frac{1}{k_{ri,j,k}} \ln\left(\frac{r_{i+1/2}}{r_i}\right) + \frac{1}{k_{ri+1,j,k}} \ln\left(\frac{r_{i+1}}{r_{i+1/2}}\right)}$	$\frac{\Delta\theta_j \Delta z_k}{\frac{1}{k_{ri-1,j,k}} \ln\left(\frac{r_{i-1/2}}{r_{i-1}}\right) + \frac{1}{k_{ri,j,k}} \ln\left(\frac{r_i}{r_{i-1/2}}\right)}$
Cylindrical, angular	$\frac{\ln\left(\frac{r_{i+1/2}}{r_{i-1/2}}\right)\Delta z_k}{\frac{\theta_{j+1/2}-\theta_j}{k_{\theta i,j,k}} + \frac{\theta_{j+1}-\theta_{j+1/2}}{k_{\theta i,j+1,k}}}$	$\frac{\ln\left(\frac{r_{i+1/2}}{r_{i-1/2}}\right)\Delta z_k}{\frac{\theta_{j-1/2}-\theta_{j-1}}{k_{\theta i,j-1,k}} + \frac{\theta_j-\theta_{j-1/2}}{k_{\theta i,j,k}}}$
Cylindrical, vertical	$\frac{\frac{\Delta\theta_j}{2}\left(r_{i+1/2}^2 - r_{i-1/2}^2\right)}{\frac{z_{k+1/2}-z_k}{k_{zi,j,k}} + \frac{z_{k+1}-z_{k+1/2}}{k_{zi,j,k+1}}}$	$\frac{\frac{\Delta\theta_j}{2}\left(r_{i+1/2}^2 - r_{i-1/2}^2\right)}{\frac{z_{k-1/2}-z_{k-1}}{k_{zi,j,k-1}} + \frac{z_k-z_{k-1/2}}{k_{zi,j,k-1}}}$
Cartesian, x-direction	$\frac{\Delta y_j \Delta z_k}{\frac{x_{i+1/2}-x_i}{k_{xi,j,k}} + \frac{x_{i+1}-x_{i+1/2}}{k_{xi+1,j,k}}}$	$\frac{\Delta y_j \Delta z_k}{\frac{x_{i-1/2}-x_{i-1}}{k_{xi-1,j,k}} + \frac{x_i-x_{i-1/2}}{k_{xi,j,k}}}$
Cartesian, y-direction	$\frac{\Delta x_i \Delta z_k}{\frac{y_{j+1/2}-y_j}{k_{yi,j,k}} + \frac{y_{j+1}-y_{j+1/2}}{k_{yi,j+1,k}}}$	$\frac{\Delta x_i \Delta z_k}{\frac{y_{j-1/2}-y_{j-1}}{k_{yi,j-1,k}} + \frac{y_j-y_{j-1/2}}{k_{yi,j,k}}}$
Cartesian, z-direction	$\frac{\Delta x_i \Delta y_j}{\frac{z_{k+1/2}-z_k}{k_{zi,j,k}} + \frac{z_{k+1}-z_{k+1/2}}{k_{zi,j,k+1}}}$	$\frac{\Delta x_i \Delta y_j}{\frac{z_{k-1/2}-z_{k-1}}{k_{zi,j,k-1}} + \frac{z_k-z_{k-1/2}}{k_{zi,j,k}}}$

$$T_{i,j,k}^n = \left(G\frac{1}{\mu B}\right)_{i,j,k}^n \tag{31}$$

where G is a geometric factor, calculated with the expressions presented in Table 2.

Equation (32) shows the independent terms vector from the linear system. Through this term, it is possible to implement internal boundary conditions and to relax gravitational hypothesis.

$$Q_{i,j,k}^{n} = -\left(\frac{\Gamma_{i,j,k}^{n+1}}{\Delta t} p_{i,j,k}^{n} + q_{sc}^{n+1} - Q_{Gi,j,k}^{n} \right) \tag{32}$$

Equation (33) shows the storage term involving changes in porosity and on the oil formation volume factor. This term accounts for the total compressibility, and it represents an "inertia" to pressure changes. The gravitational term is written as:

$$\Gamma_{i,j,k}^{n+1} = V_b \frac{\phi^{n+1} c_t}{B^{n+1}} \tag{33}$$

$$\begin{aligned} Q_{Gi,j,k}^{n} &= A_{Gi,j,k}^{n} Z_{i,j,k+1} + B_{Gi,j,k}^{n} Z_{i,j,k-1} + N_{Gi,j,k}^{n} Z_{i,j+1,k} \\ &+ S_{Gi,j,K}^{n} Z_{i,j-1,k} + W_{Gi,j,k}^{n} Z_{i-1,j,k} + E_{Gi,j,k}^{n} Z_{i+1i,j,k} + C_{Gi,j,k}^{n+1} Z_{i,j,k} \end{aligned} \tag{34}$$

The term expressed in Equation (34) term takes into account the influence of the hydraulic load of the neighboring cells, similarly to the Equation (23). The coefficients multiplying pressures are defined as following:

$$A_{Gi,j,k}^{n} = A_{i,j,k}^{n} \gamma_{i,j,k+1/2}^{n+1} \tag{35}$$

$$B_{Gi,j,k}^{n} = B_{i,j,k}^{n} \gamma_{i,j,k-1/2}^{n+1} \tag{36}$$

$$N_{Gi,j,k}^{n} = N_{i,j,k}^{n} \gamma_{i,j+1/2,k}^{n+1} \tag{37}$$

$$S_{Gi,j,k}^{n} = S_{i,j,k}^{n} \gamma_{i,j-1/2,k}^{n+1} \tag{38}$$

$$W_{Gi,j,k}^{n} = W_{i,j,k}^{n} \gamma_{i+1/2,j,k}^{n+1} \tag{39}$$

$$E_{Gi,j,k}^{n} = E_{i,j,k}^{n} \gamma_{i-1/2,j,k}^{n+1} \tag{40}$$

$$C_{Gi,j,k}^{n+1} = -\left(A_{Gi,j,k}^{n} + B_{Gi,j,k}^{n} + N_{Gi,j,k}^{n} + S_{Gi,j,k}^{n} + W_{Gi,j,k}^{n} + E_{Gi,j,k}^{n} \right) \tag{41}$$

3. Methodology

Plots of the pressure variation from the initial pressure within a distance from the wellbore and time from the production beginning were drawn through the usage of the Mathematica Wolfram Software language. The plots will only relate the variation of pressure to time or distance individually, while the other variable is kept constant. It is useful to define the pressure variation in order to accomplish that:

$$\Delta p = p_i - p = \frac{q_w \mu}{4\pi kh} E_i \left(\frac{\phi \mu c_t r^2}{4kt} \right) \tag{42}$$

It is necessary a brief discussion of what this new parameter represents in terms

of oil production and why it is important.

Higher pressure variations within the time for a fixed point for two similar reservoirs implies that the one with higher pressure variation has less energy stored for oil elevation, which is undesirable economically and technically for production. Hence, it is desirable that the reservoir parameters generate smaller pressure drops within the time from a production point of view so that it is possible to maintain the oil production.

Naturally, it is desirable that the reservoir shows smaller pressure variation and pressure gradient values on points further away from the well for a fixed time.

Assuming monophasic flow with no fluid injection through the reservoir limits, the flow regime will evolve to pseudo-permanent, since there is no fluid influx to the reservoir. Therefore, pressure drops will not be balanced through the reservoir limits. The flow rate through the wellbore is assumed constant, therefore bigger pressure variations means there will be less fluid volume produced.

The standard values of reservoir parameters are listed in the Table 3.

Table 3. Reservoir parameters original values [3].

Parameter	Value	Unity
Permeability	$9{,}87 \times 10^{-14}$	m^2
Viscosity	3×10^{-3}	$Pa.s$
Production flow rate	35	m^3/day
Rock formation depth	4	m
Porosity	0,2	Non-dimensional
Compressibility	$1{,}33 \times 10^{-9}$	Pa^{-1}
Well radius	0,1	m

The results are displayed by plotting the pressure against either distance from the wellbore center or time, keeping the other variable constant. The chosen fixed distance and time values are 300m and 30 days. A set of five plots were generated to study each parameter with five different parameters values ranging from usual values found on the field to discuss the influence that each parameter bears on the behavior of the flow.

Following, Equations (23) to (41) are implemented in Mathematica and the FDM model is validated by comparison with the analytical solution curves. The fixed values of distance and time are set to t = 10 days and r = 300 meters. The initial pressure is set to zero in order to obtain the pressure variation instead of the pressure in the reservoir, and the final answer is the negative of the output generated by the method. The analytical model is used to obtain the distance from the center of the wellbore for which the pressure variation is less than 0.1kPa to simulate and infinite dimension reservoir (a reservoir in transient flow conditions). The extension of the grid goes

from the well radius until that radius and the last cells are set to remain at the initial pressure conditions all the time. The constant rate well is modeled through the source/sink term in Equation (32). The grid generated has $(n_\theta \times n_r \times n_z) = (900 \times 4 \times 4)$ cells, and $n_t = 200$ ($\Delta t = 0.05$ days) . The values of porosity and oil formation volume factor are updated by applying Equations (12) and (13). The viscosity is not updated at the end of every time-step, since it's values are reasonably constant with pressure variations for oils with no gas dissolved [5].

After the model validation, the hypothesis regarding no gravitational effects is relaxed and the analytical solution is compared with the new solution.

The next step is to keep hypothesis regarding no gravitational effects and to impose a pseudorandomly distributed permeability through the mesh and compare the new solution to the analytical one again.

At the end, gravitational effects and permeability hypothesis are simultaneously relaxed (using the same permeability values generated) and the final solution is compared to the analytical solution.

4. Results

Figs. 1 and 2 are plotted following the procedure listed in the methodology section with respect to the analytical solution of the Diffusivity Equation. Figure 1 brings the pressure variation plotted against distance and fixed in time, and Figure 2 plots pressure variation against time for a fixed distance to the wellbore.

Fig. 1a shows the original solution within time and plot 1b plots the original solution within distance. At the beginning, the entire reservoir is at the same pressure $p_{t=0}$. When the production starts, the pressure begins to fall. At first, the pressure measured at a point sufficiently far from the center of the wellbore (which might be relatively close to the wellbore) will remain with the initial pressure for a certain time, without the influence of the production. The pressure on that point starts to drop after a sufficiently long time. The boundary conditions do not affect the entire fluid mass immediately; this is a particular quality of the transient flow regime. The model will show null pressure variation on that point if not enough time is waited. As the boundary conditions travel through the reservoir, the pressure variation starts to increase and it is bigger closer to the wellbore. The radius variation is more significant on the values that the pressure variation will assume, since it appears with a higher exponent than the time. This explains the basic behavior of the pressure variation.

Fig. 1b and Fig. 2b show the solutions for different permeability values. The bigger the fluid permeability, the lower it will take to move the fluid to the surface. This results in in small pressure variations, and it will be possible to keep the flow for a longer period. In addition, the boundary conditions imposed will travel to the limits of the reservoir faster, which implies higher pressure variation values at the beginning when comparing to reservoirs with smaller permeability. Moreover, the reservoir will change its flow regime faster. Fig. 1b shows that the pressure variation grows faster for higher permeability values at the beginning of the production, and reach smaller values for longer periods. Fig. 2b shows that the pressure variation is much smaller for higher permeability values along the reservoir extension for a fixed time.

Fig. 1c and 2c show the solutions with different viscosity values. The fluid viscosity has the opposite effect of the permeability of the pressure variation. The

flow in the direction of the well demands more energy for highly viscous fluids because of the increase of the energy lost due to friction. That means the pressure variation will be higher for viscous fluids, supposing constant flow rates. At the beginning of the production, however, the pressure variation will be smaller for highly viscous fluids. That happens because the pressure drop due to the production start propagates slower to the reservoir extension. Fig. 1c shows that the pressure variation increases faster for more viscous fluids at the beginning of the production, and it is soon exceeded by the curves of less viscous fluids. Fig. 2c shows that less viscous fluids cause smaller pressure variation values along the reservoir extension for a fixed time.

Fig. 1d and 2d show the solutions with different rock formation depth values. Deeper rock formations have bigger drained areas. In the case of vertical wells, it is necessary less energy to make a bigger fluid volume flow inwards the well and the pressure variation will be smaller. It is a good solution to build horizontal wells when dealing with shallow rock formations, because the draining area will be larger, and a smaller number of the well will be necessary for a feasible production. Pressure Variation is proportional to the inverse of rock formation depth. Plotting both variables on the same plane would result in a hyperbole. Fig. 1d shows that the pressure variation increases fast for shallower rock formations within time and much slower and smoother for deeper formations. Fig. 2d shows that deeper rock formation depth implies better results for the pressure variation along the reservoir extension.

Fig. 1e and Fig. 2e show the solution for different porosity values. It is assumed that the increase of porosity is homogeneously distributed in the rock formation for this analysis. Pores that create vertical paths are irrelevant to the radial flow, whereas pores that create continuous radial paths increases the flow easiness. This means that the increase of pores has a similar effect to that of the increase of the permeability, but with a smaller intensity. Therefore, a porosity increase implies a pressure variation decrease. Fig. 1e shows that the pressure variation in time is smaller for reservoirs that are more porous, and Fig. 2e shows that the pressure variation is also smaller for more porous reservoirs within distance since it is easier to move oil from any point of the reservoir to the wellbore.

Fig. 1f and Fig. 2f show the solution or different compressibility values. The total compressibility can be regarded as a measure of the amount of energy that the rock and fluid may be stored in the form of potential energy through deformation. The pressure drop travels along the reservoir and decompresses both fluid and rock when the production starts. The fluid and the rock expand and mitigate the pressure drop during the decompression. In addition, the high value of compressibility means there will be more energy for the fluid elevation stored in the reservoir, which makes the pressure variation smaller. Fig. 1f shows that, for smaller compressibility values, the pressure variation is bigger, which implies that more energy is spent. Fig 2f shows that the pressure variation along the extension of the reservoir is bigger for smaller compressibilities; therefore, more energy is spent to move the fluid from a certain point in the reservoir to the wellbore.

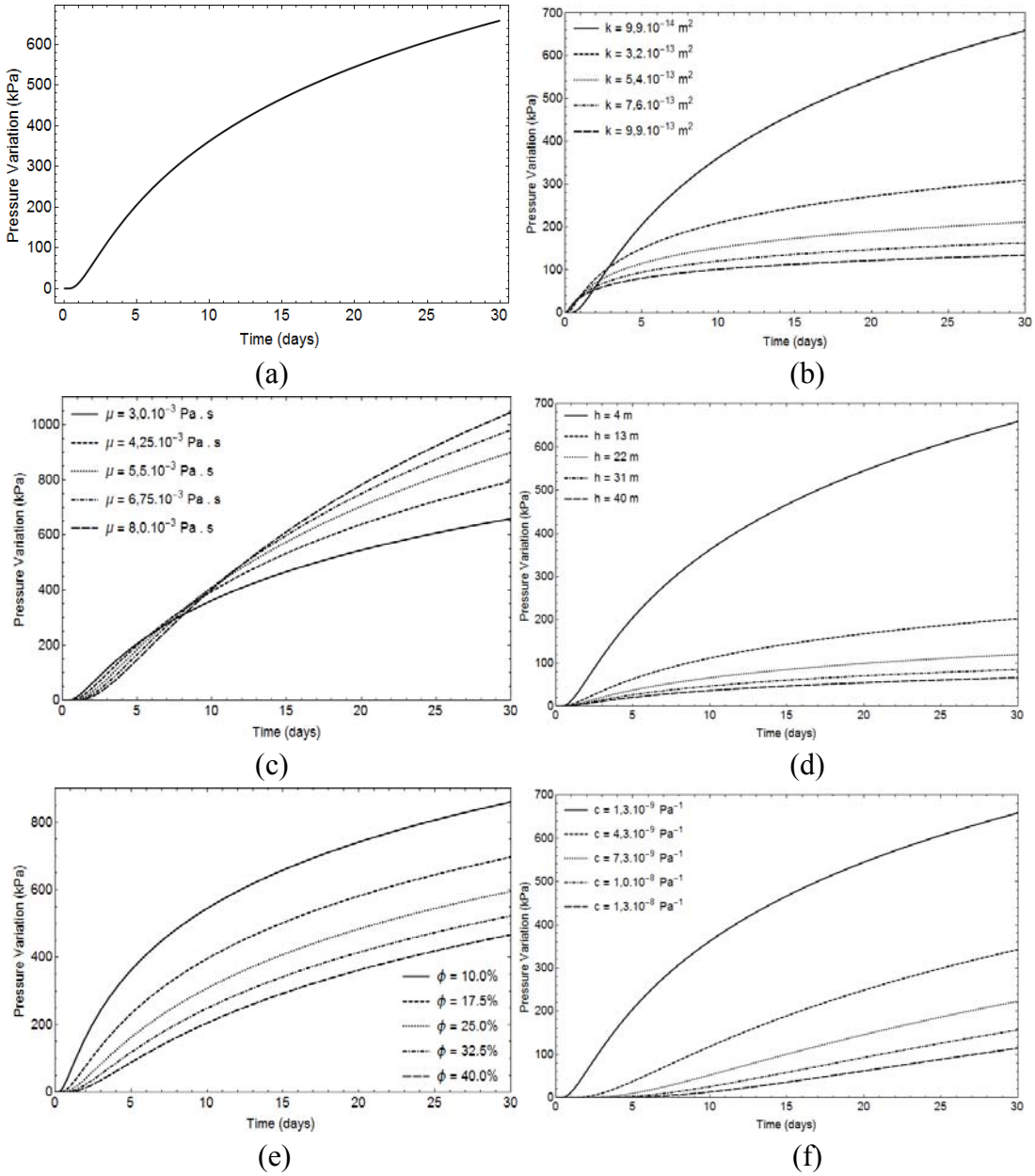

Fig. 1. Pressure variation within time for r = 300 m; (a) Original solution; (b) different permeability values; (c) different viscosity values; (d) different rock depth values; (e) different porosity values; (f) different compressibility values.

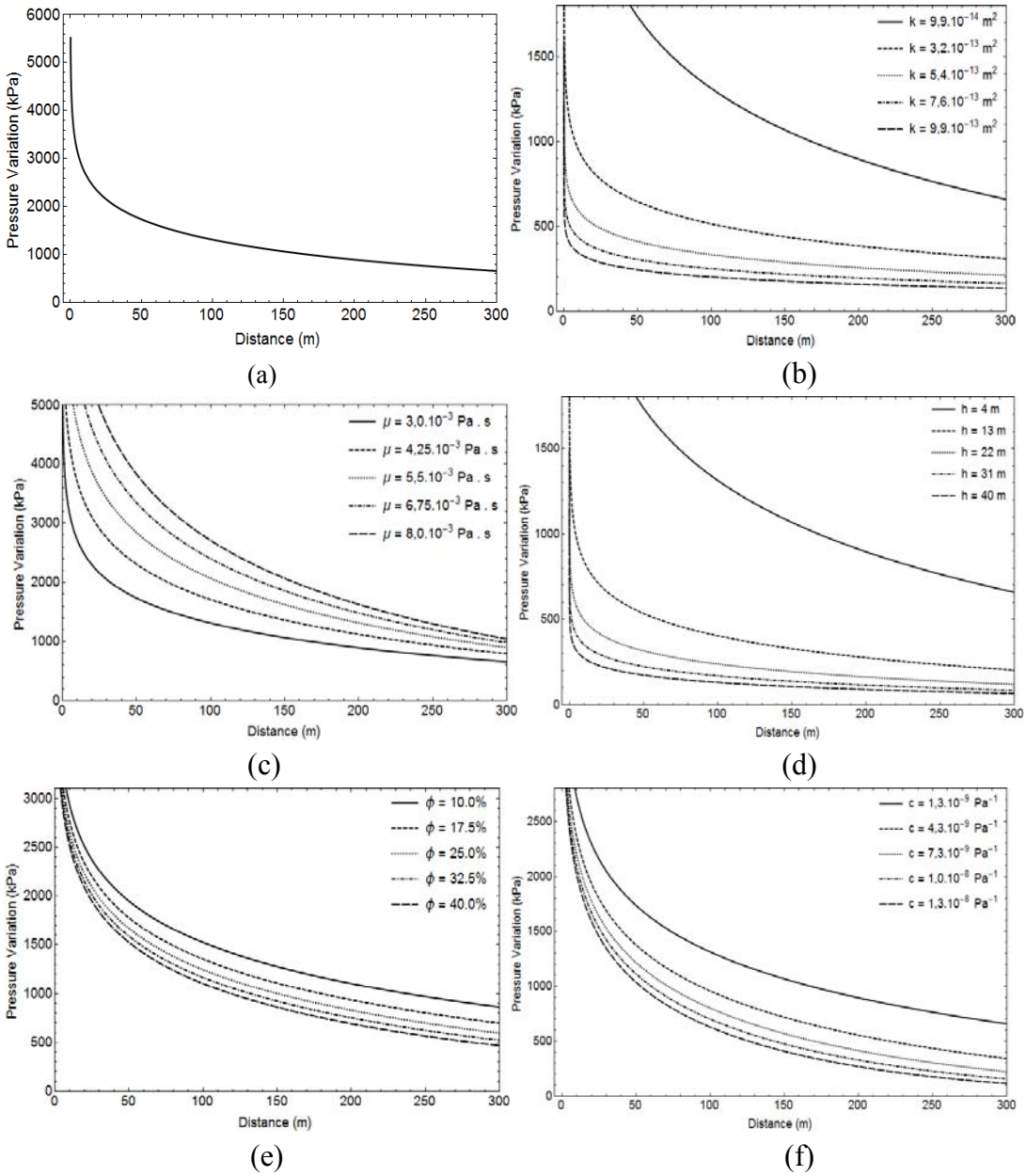

Fig. 2. Pressure variation within distance for t=30 days; (a) Original solution; (b) different permeability values; (c) different viscosity values; (d) different rock depth values; (e) different porosity values; (f) different compressibility values.

In summary, the permeability, higher values of rock formation depth, porosity, and total compressibility favors the production, while the viscosity disfavors it.

5. FDM Validation

Fig. 3, 4, 5, 6 of the numerical model are generated, continuing the steps listed in the methodology section. Fig. 3 is used for the validation of the model, while Fig. 4 and 5 are used to relaxed gravitational and permeability hypothesis individually and Fig. 6 shows the results when both hypotheses are relaxed.

The value of the radius that accomplishes the required is around 2500m is found using the procedure described in the methodology section to find the distance where pressure variation is smaller than 0.1kPa. However, the external radius adopted was 3000m, as it was possible to simulate a bigger radius without much increase in computational cost.

It is clear that the numerical model estimates the values of the analytical solution with minimal errors from Fig. 3a and Fig. 3b. Indeed, if the biggest absolute deviation is taken from the two cases and each of them is divided by the respective average value of the analytical solution on the intervals calculated, the ratios are 4.4% e 1.5%. In reality, the biggest absolute deviations occur on plot regions where the actual analytical pressure variation values are much bigger than the average pressure variation value; hence, the two percentages values obtained are actually overestimation of the deviation.

Higher oscillation on the numerical solution is observed next to the wellbore. That may be justified by the high-pressure variation gradient values next to the well, which causes some numerical instability. Overall, the numerical approximation is good.

The numerical solution is slightly displaced when relaxing the gravitation hypothesis as can be seen in Fig. 4a and Fig. 4b.

However, there is still no vertical flow, since the rock formation is horizontal. The displacement is caused because now, when specifying the initial condition on the program input, it is the initial fluid flow potential that is being specified, but the calculations are still aiming to obtain the pressure conditions. The pressure must be lesser than when calculated for no gravitational effects as both pressure and height values are positive and the fluid flow potential is the value that the pressure was supposed to be. The pressure variation is obtained by taking the negative values of the solution as it was stated in the methodology section. In other words, the pressure variation must be bigger because the pressure obtained is smaller than the previous value.

Fig. 5a and Fig. 5b are plotted by returning the gravitation hypothesis and imposing a pseudorandomly distributed permeability.

This hypothesis, so far, is shown to be the one that most introduces error to the analytical model hypothesis. However, that depends on how other reservoir natural characteristics are, of course. For example, if the rock formation had greatly varying height variations, it is possible that the gravitational effect would play a more important role. Nevertheless, in this case, the analytical model is shown to be ineffective for reasonable estimations of the pressure variation values of an anisotropic and heterogeneous permeability distribution. On the other side, the qualitative behavior is still the same.

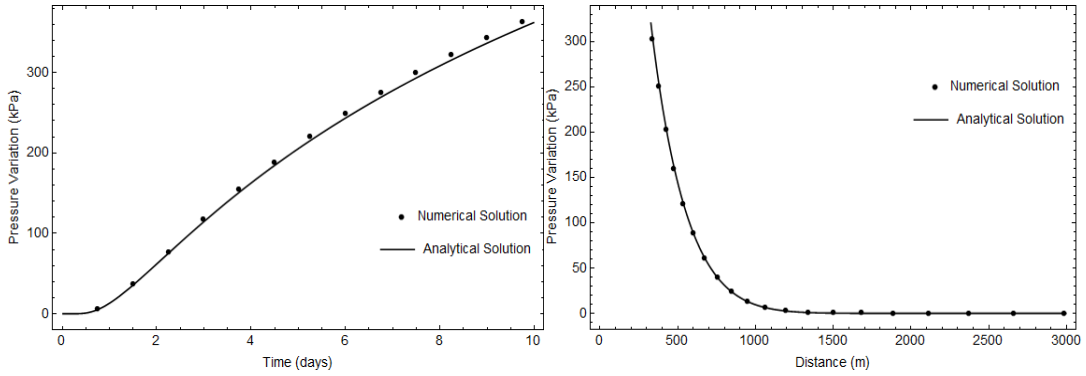

(a) (b)

Fig. 3. Validation of the numerical model. (a) validation for the fixed in distance solution (r=300m); (b) Validation for the fixed in time solution (t= 10 days).

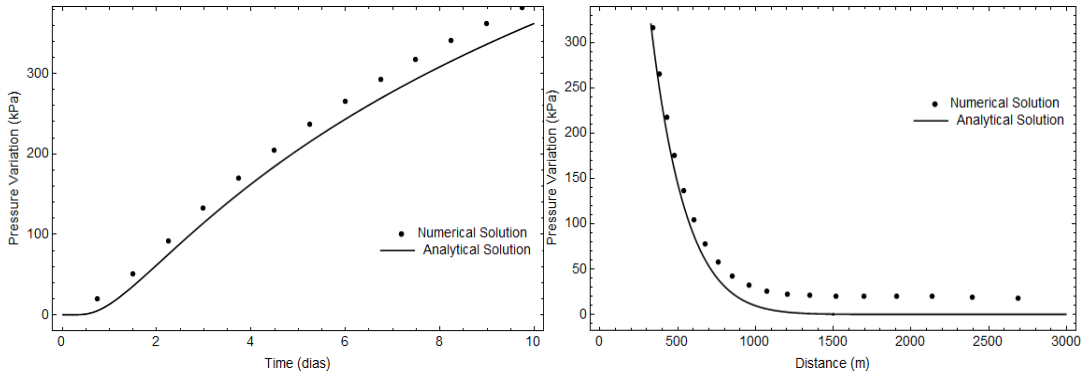

(a) (b)

Fig. 4. Relaxing gravitation hypothesis. (a) pressure variation plotted against time; (b) pressure variation plotted against distance.

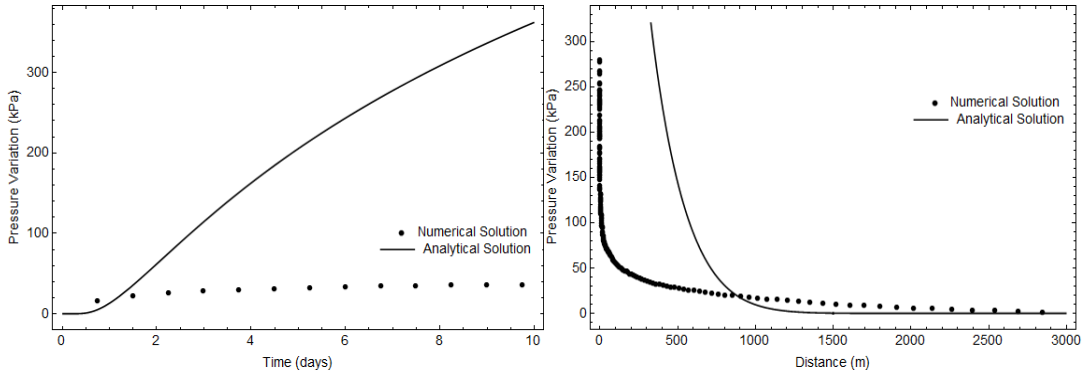

(a) (b)

Fig. 5. Relaxing permeability hypothesis; (a) pressure variation plotted against time; (b) pressure variation plotted against distance.

One gets Fig. 6a and Fig. 6b by relaxing both hypotheses of the previous two sections simultaneously.

The behavior of the numerical solution has changed further than the superposition of effects of the two relaxations. This is a consequence of the non-linearity of the Diffusivity Equation.

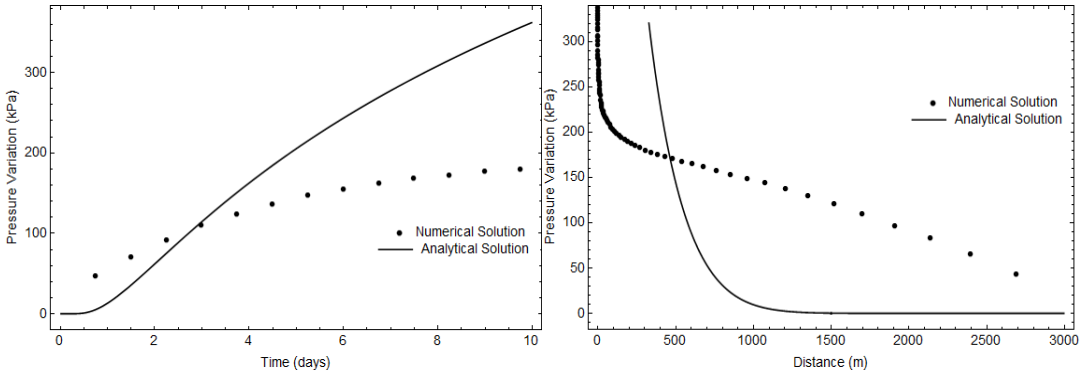

(a) (b)

Fig. 6. Relaxing both gravitation and permeability hypothesis; (a) pressure variation plotted against time; (b) pressure variation plotted against distance.

6. Conclusions

The pressure variation analysis within the various parameters from the solution of Diffusivity Equation for a radial, transient flow is one of the starting points of the viability study.

It is concluded that rock thickness, intrinsic permeability, reservoir total compressibility, and porosity mitigates the energy demanded to elevate the oil, while viscosity enhances the energy loss by analyzing each of the parameters present in the analytical solution of the Equation (16). The explanation for why each of these variables causes the effects listed follows the curves for each individual parameter results.

The numerical model was successful validated, and its results showed reasonably low errors. It is clear that the permeability hypothesis showed a greater influence on the numerical solution deviation from the analytical solution when comparing the results of relaxing gravitational and permeability hypothesis individually. The curve deviation obtained cannot be seen as a superposition of effects of both effects individually when both hypotheses were relaxed simultaneously, because of the equation's non-linear behavior.

In addition, it is possible to conclude that the analytical model might not represent correctly a more complex reservoir; however, it can be used to qualitatively study the behavior of oil reservoirs.

Acknowledges

The authors acknowledge the support of the following agencies: the National Council for Scientific and Technological Development (CNPq-Project 30449420127), the Coordination for the Improvement of Higher Level Personnel (CAPES-Project 1431/14-5), and the University of Brasilia for funding this research.

References

[1] I. Wolfram Research, Mathematica, Version 10.1 ed., Champaign, Illinois: Wolfram Research, Inc, 2015.

[2] T. Ahmed. Reservoir Engineering Handbook, United States: Elsevier, 2010.

[3] A. J. Rosa, R. d. S. Carvalho e J. A. D. Xavier. Engenharia de Reservatório de Petróleo, Brazil: Interciência, 2006.

[4] A. Szymkiewicz. Modelling Water Flow in Unsaturated Porous Media, Poland: Springer, 2013.

[5] T. Ertekin, H. A.-K. Jamal e R. K. Gregory. Basic Applied Reservoir Engineering, United States: Society of Petroleum Engineers, 2001.

[6] R. Firoozabadi, F. Sonier. Numerical simulation of complex reservoir problems and the need for a different line of attack. The Way Ahead, 2007, 3(3): 17-19.

[7] K. Aziz e O. A. Pedrosa. Use of Hybrid Grid in Reservoir Simulation. SPE Reservoir engineering, 1986, 1(6), 611-621.